

Rational Design of Antibody Protease Inhibitors

Tao Liu,[†] Guangsen Fu,[‡] Xiaozhou Luo,[†] Yan Liu,[‡] Ying Wang,[‡] Rongsheng E. Wang,[†]
Peter G. Schultz,^{*,†,‡} and Feng Wang^{*,‡}

[†]Department of Chemistry and the Skaggs Institute for Chemical Biology, The Scripps Research Institute, La Jolla, California 92037, United States

[‡]California Institute for Biomedical Research (Calibr), La Jolla, California 92037, United States

Supporting Information

ABSTRACT: The bovine antibody BLV1H12, which has an ultralong CDR3H, provides a novel scaffold for engineering new functions into the antibody's variable region. By modifying the β -strand "stalk" of BLV1H12 with sequences derived from natural or synthetic protease inhibitors, we have generated antibodies that inhibit bovine trypsin and human neutrophil elastase (HNE) with low nanomolar affinities. We were able to generate a humanized variant using a human immunoglobulin scaffold that shares a high degree of homology with BLV1H12. Further optimization yielded a highly selective humanized anti-HNE antibody with sub-nanomolar affinity. This work demonstrates a novel strategy for generating antibodies with potent and selective inhibitory activities against extracellular proteases involved in human disease.

The human genome encodes over 270 extracellular proteases with diverse functions.¹ Selective inhibitors of these proteases are important tools for determining their physiological functions, as well as potential therapeutics for the treatment of human disease. Although many small-molecule protease inhibitors have been generated, their use *in vivo* requires optimization of selectivity and pharmacokinetic properties, which can be quite time-consuming. Monoclonal antibodies afford an alternative strategy for generating high-affinity and selective binders to virtually any macromolecule; they also have relatively long half-lives which facilitate their use *in vivo*. There are several reports on the generation of antibodies that inhibit proteases.² One approach involves immunization and subsequent screening for neutralizing antibodies. Recently, panning of phage-displayed human antibody libraries (more recently combined with computational design) has also been used to identify human antibodies that are protease inhibitors.^{3–9}

Interestingly, among these antibodies, the ones with longer than normal heavy-chain complementary determining region 3 (CDR3Hs) were found to inhibit proteases by inserting the long CDR3H into the active-site cavity^{3,9} in a similar fashion to natural polypeptide-based protease inhibitors.¹⁰ We recently discovered a subgroup of antibodies in the bovine antibody repertoire with exceptionally long CDR3H loops. The X-ray crystal structure of one such antibody, BLV1H12, revealed a novel structural feature in which CDR3H folds into a disulfide cross-linked "knob" domain fused to an antiparallel β -stranded

"stalk", which is ~ 20 Å in length and highly solvent-exposed (Figure 1A).¹¹ This β -strand-forming sequence evolves during

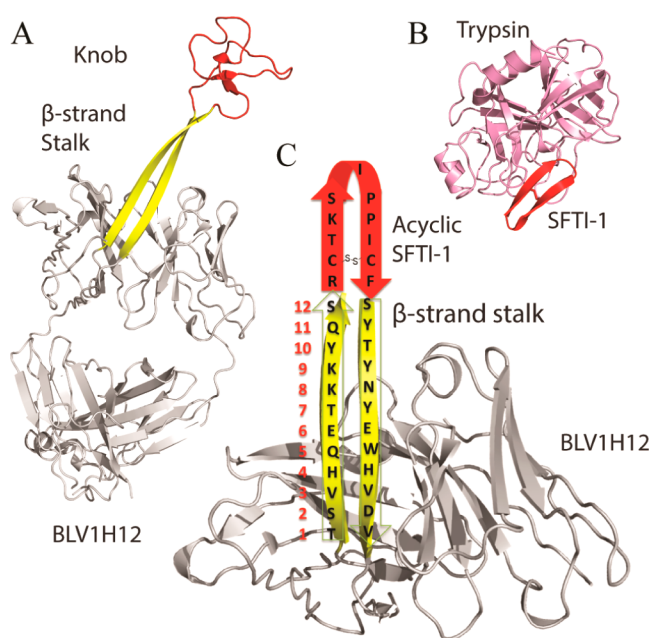


Figure 1. (A) Crystal structure of bovine antibody BLV1H12 Fab (PDB code 4K3D), showing a disulfide cross-linked "knob" domain (red) supported by a β -strand "stalk" (yellow). (B) Co-crystal structure of cyclic peptide SFTI-1 (red) and trypsin (pink) complex (PDB code 1SFI). (C) Graphical representation of anti-trypsin antibody design. The active β -hairpin loop of SFTI-1 (red) was fused with the evolutionarily conserved β -strand "stalk" (yellow) of antibody BLV1H12 to replace the "knob" domain. The length of stalk is indicated by the number of residues.

VDJ rearrangement and B cell maturation and is conserved in most of the bovine antibodies with ultralong CDR3Hs. Interestingly, such double-stranded antiparallel β -sheet structures are also commonly found in natural protease inhibitors.^{12,13} For example, sunflower trypsin inhibitor-1 (SFTI-1), the smallest Bowman–Birk inhibitor family member, adopts a double-stranded antiparallel β -hairpin conformation that is stabilized by a disulfide bridge (Figure 1B).¹⁴ The co-crystal structure of SFTI-1 bound to trypsin reveals a competitive inhibition mode

Received: December 23, 2014

Published: March 16, 2015

wherein the extended β -strand of SFTI-1 occupies the P1–P4 sites of the protease active site to form a non-covalent tight-binding complex.¹⁵ In fact, such a binding mode between proteases and the extended β -strands of peptide ligands is common to canonical serine protease inhibitors¹⁶ and can also be found in other protease inhibitor families.^{17,18} We have previously shown that peptides which adopt an antiparallel β -hairpin structure can be engineered into the structurally unique CDR3H region of bovine antibody BLV1H12 to replace the knob domain while still maintaining an active conformation.¹⁹ Thus, we asked if we can use a similar strategy to generate antibodies that bind and inhibit proteases.

As a first step in this direction, we attempted to generate a bovine antibody inhibitor of trypsin (bAb-TI) by replacing the knob domain of BLV1H12 with the disulfide-bridged cyclic loop of SFTI-1 (Figure 1C). Briefly, the acyclic β -hairpin region derived from SFTI-1 (RC*TKSIPPIC*F, where C*C* represents a disulfide bond) was substituted into the CDR3H region in place of the knob domain such that the N- and C-termini of the peptide were directly fused with the ascending (TSVHQETKKYQS) and descending (SYTYNYEWHVDV) β -strands of the “stalk”. The designed antibody Fab was transiently expressed in 293-F cells with a hexahistidine tag at the C-terminus of the heavy chain. The antibody was secreted into expression medium and purified by Ni-NTA resin with a yield of 15 mg/L. The purified protein could be concentrated to >10 mg/mL in PBS (pH 7.4) without aggregation. SDS-PAGE analysis revealed that the antibody Fab was >90% pure and migrated as a single band around 50 kDa. In the presence of reducing reagent dithiothreitol (DTT), the heavy and light chains of the fusion protein migrated at ~30 and 25 kDa, respectively (Figure 2A). The identity of bAb-TI was further confirmed by electrospray ionization mass spectrometry (ESI-MS) (Supporting Information, Figure S1).

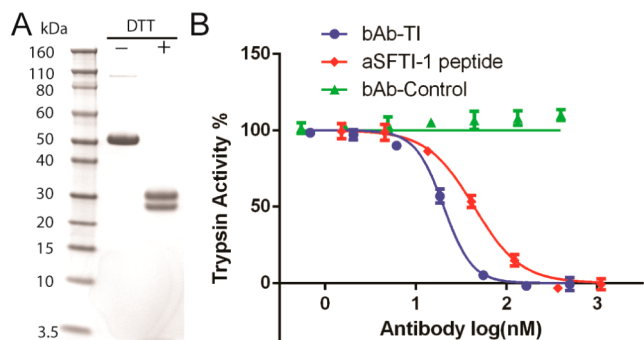


Figure 2. (A) SDS-PAGE gel of purified bAb-TI Fab in the absence (–) or presence (+) of reducing reagent DTT. (B) Anti-trypsin antibody bAb-TI potently inhibits trypsin activity. Bovine pancreatic trypsin at 40 nM was incubated with increasing concentrations of bAb-TI, acyclic SFTI-1 peptide, or a bAb control antibody for 15 min, followed by the addition of 40 μ M fluorescent substrate Bz-Arg-AMC. Residual enzyme activity was monitored using a plate reader (EX 380 nm/EM 460 nm). Assays were performed in triplicate.

Next, we determined whether the antibody bAb-TI inhibits the protease activity of trypsin. Bovine pancreatic trypsin (40 nM) was incubated with increasing concentrations of bAb-TI for 15 min, and residual enzyme activity was measured using Bz-Arg-AMC as the substrate. As shown in Figure 2B, bAb-TI potently inhibits trypsin in a concentration-dependent manner, whereas the control antibody BLV1H12 showed no activity up to 1 μ M.

Fitting the data using a tight-binding equation²⁰ gave $K_i = 3.80 \pm 1.88$ nM. For comparison, the disulfide-bridged monocyclic SFTI-1 peptide aSFTI-1 (with the sequence GRC*TKSIPPIC*FPD, where C*C* represents a disulfide bond) was synthesized and assayed in parallel with the antibody inhibitor. The K_i value of aSFTI-1 for trypsin was determined to be 14.3 ± 3.7 nM, consistent with a literature value.¹⁴ This result indicates that bAb-TI is ~4-fold more potent than the nonfused peptide, suggesting that the antibody scaffold supports the correct folding of the peptide into its active antiparallel β -hairpin conformation.

To determine the binding affinity and kinetics between the antibody and antigen, a biolayer interferometry experiment was performed using an Octet RED instrument (ForteBio, Inc.). Briefly, His-tagged bAb-TI was immobilized onto a Ni-NTA-coated biosensor and incubated with various concentrations of trypsin. The k_{on} and k_{off} values, measured in real time at room temperature, were determined to be $9.68 \times 10^4 \pm 0.05 \times 10^4$ $M^{-1}s^{-1}$ and $3.26 \times 10^{-4} \pm 0.07 \times 10^{-4}$ s^{-1} , respectively (Figure S2). The calculated dissociation constant (K_d) between bAb-TI and trypsin was determined to be 3.37 ± 0.07 nM, consistent with the K_i value obtained from the trypsin inhibition assay.

To demonstrate the utility and generality of this approach, we next attempted to generate antibodies against human neutrophil elastase (HNE). HNE is a serine protease secreted by neutrophils and macrophages during inflammation; it is a therapeutic target for the development of anti-inflammatory drugs.²¹ To generate antibodies against HNE, a disulfide-bridged peptide elastase inhibitor, HNEI (with a sequence MC*TASIPPQC*Y, where C*C* represents a disulfide bond), originally identified from a combinatorial peptide library,²² was inserted onto the CDR3H stalk of bovine antibody BLV1H12 (in a fashion similar to bAb-TI) to yield elastase inhibitor bAb-EI-L12 (L12 indicates that the β -strand linker is 12 residues in length, as shown in Figure 1C). In addition, a second anti-HNE antibody, bAb-EI-L9, was designed by shortening the β -strand linker of bAb-EI-L12 by three residues on each strand, starting from the peptide–linker junction (the resulting CDR3H sequences are shown in Table 1). Both antibody Fabs were expressed, purified, and characterized as described above (Figure S3). The final yields after purification were >15 mg/L for each protein.

The activities of the antibodies were measured by incubating increasing concentrations of bAb-EI with 20 nM HNE for 15 min at room temperature, and residual enzyme activities were analyzed using the fluorogenic elastase substrate MeOSuc-AAPV-AMC. Both antibodies potently inhibit HNE activities, with $K_i = 19.0 \pm 2.2$ and 19.9 ± 2.3 nM for bAb-EI-L12 and bAb-EI-L9, respectively, whereas the control antibody BLV1H12 showed no inhibition (Figure S4 and Table 1). For comparison, the parent HNEI peptide was assayed in parallel, giving $K_i = 91.8 \pm 9.7$ nM, consistent with the published result.²² These experiments again show that the antibodies are ~4-fold more potent than the original peptide, supporting the notion that the antibody scaffold helps to correctly fold the peptide into its active conformation. The binding affinities between antibodies and HNE were also measured by Octet binding assay, and $K_d = 13.3 \pm 0.98$ and 9.57 ± 0.30 nM for bAb-EI-L12 and bAb-EI-L9, respectively.

One potential obstacle that could limit the therapeutic use of these engineered bovine antibodies is a human host immune response stimulated by the bovine-derived antibody scaffold. A protein structure homology search identified a humanized antibody, HuLys²³ (PDB code 1BVK), specific for hen egg-white lysozyme binding,²⁴ that shows a high degree of homology

Table 1. CDR3H Sequences of Designed Anti-HNE Antibodies and Their Potency against HNE

antibody	CDR3H sequence ^a	K_i (nM) ^b	K_d (nM) ^c
bAb-EI-L12	TSVHQETKKYQS-MC*TASIPPQC*Y-SYTYNIEWHVDV	19.0 ± 2.2	13.3 ± 1.0
bAb-EI-L9	TSVHQETKK-MC*TASIPPQC*Y-YNYEWHVDV	19.9 ± 2.3	9.57 ± 0.30
hAb-EI-L4	TSVH-MC*TASIPPQC*Y-HVDV	58.1 ± 6.2	ND
hAb-EI-L5	TSVHQ-MC*TASIPPQC*Y-WHVDV	4.49 ± 1.07	2.15 ± 0.09
hAb-EI-L6	TSVHQE-MC*TASIPPQC*Y-EWHVDV	4.67 ± 1.87	2.00 ± 0.12
hAb-EI-L7	TSVHQET-MC*TASIPPQC*Y-YEWHVDV	0.83 ± 0.31	0.79 ± 0.09
hAb-EI-L8	TSVHQETK-MC*TASIPPQC*Y-NYEWHVDV	0.98 ± 0.23	0.95 ± 0.13
hAb-EI-L9	TSVHQETKK-MC*TASIPPQC*Y-YNYEWHVDV	14.6 ± 2.0	6.68 ± 0.21
hAb-EI-L7-AA	TSVHQET-MATASIPPQAY-YEWHVDV	ND	ND

^aAsterisks indicate disulfides. ^b K_i values were measured by HNE inhibition assay. ^c K_d values were measured by Octet binding assay. ND indicates the binding is too weak to accurately determine the binding constant.

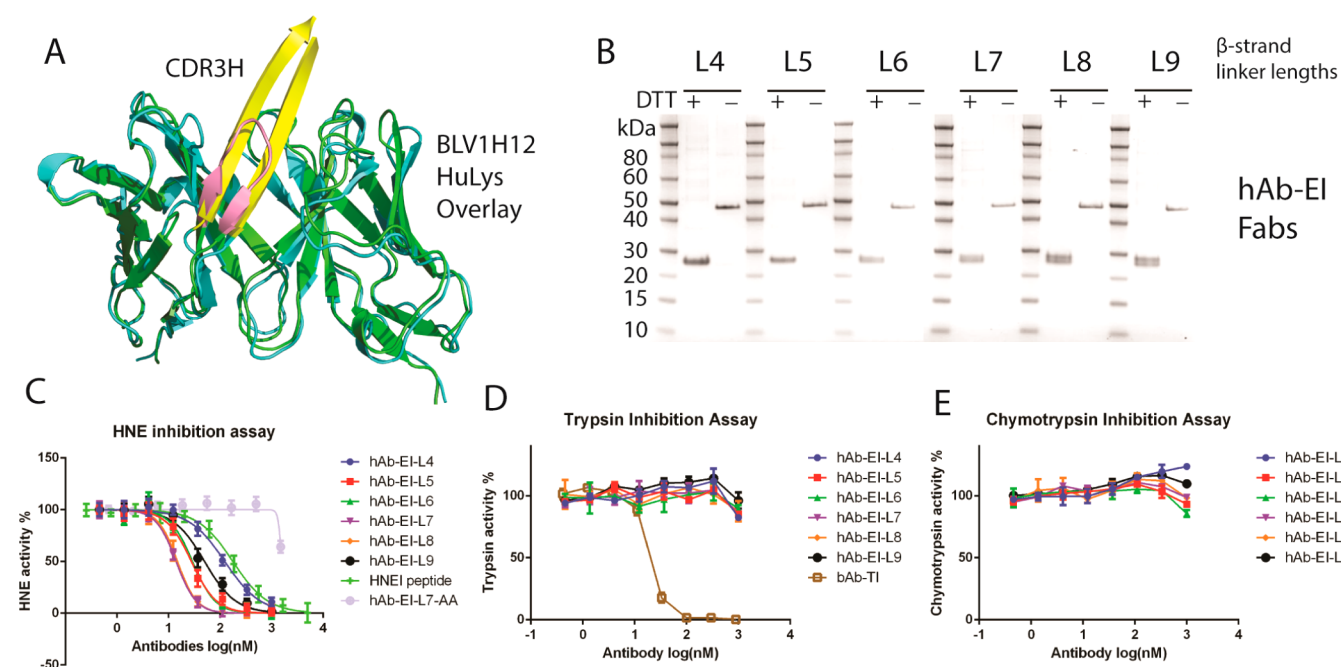


Figure 3. (A) Crystal structure alignment of BLV1H12 (cyan, PDB code 4K3D) and a humanized antibody, HuLys (green, PDB code 1BVK), sharing a high degree of structure homology. The CDR3H loop of HuLys is shown in pink, and the β -strand stalk of BLV1H12 is marked in yellow. The RMS value of alignment is 0.893 (calculated in PyMOL). (B) SDS-PAGE gel of purified hAb-EI Fabs with different lengths of β -strand stalks in the absence (–) or presence (+) of reducing reagent DTT. Antibodies were assayed against three related serine proteases sharing a high degree of structure homology: (C) human neutrophil elastase, (D) trypsin, and (E) chymotrypsin. HNE at 20 nM, trypsin at 40 nM, and chymotrypsin at 10 nM were incubated with increasing concentrations of antibodies or peptide for 15 min, followed by addition of the corresponding fluorescent substrate MeOSuc-AAPV-AMC (100 μ M), Bz-Arg-AMC (40 μ M), or Suc-AAPF-AMC (100 μ M), respectively. Residual enzyme activity was monitored using a plate reader (EX 380 nm/EM 460 nm). Assays were performed in duplicate.

to BLV1H12 in overall tertiary structure¹¹ (Figure 3A), making it an excellent candidate for generating a humanized anti-HNE antibody. To do so, the active CDR3H hairpin loop of bAb-EI-L9 (Thr96–Val124) was grafted onto the HuLys scaffold to replace the original CDR3H loop (Ala96–Tyr105) based on sequence alignment. The resulting antibody was designated as hAb-EI-L9 (human anti-elastase inhibitory antibody with a β -strand linker nine residues in length). In addition, we generated fusions with shorter linkers (hAb-EI-L8 to hAb-EI-L4) to explore the effects of linker length on binding affinity (the corresponding CDR3H sequences are listed in Table 1). All six Fabs were expressed in mammalian cells, with yields after purification \geq 5 mg/L. The antibodies were characterized by both SDS-PAGE analysis (Figure 3B) and ESI-MS (Figures S5–S10) to confirm their purities and identities. Their potency against HNE was determined by both enzyme inhibition assay (Figure 3C) and Octet binding assay (Figure S11), and the results are summarized

in Table 1. An increase in activity was observed by shortening the linker length from nine to seven residues, and the resulting hAb-EI-L7 showed the highest potency against HNE, with $K_i = 0.83 \pm 0.31$ nM and a binding affinity of 0.79 ± 0.09 nM, significantly more potent than the parent peptide (\sim 100-fold). This increased affinity may be due to conformational effects or additional favorable interactions between the protease and CDR loops. A further reduction in linker length from seven to four residues resulted in a decrease in binding affinity and potency, likely due to unfavorable steric interactions with the other CDR loops.

We next carried out a mutagenesis study on the other CDRs of hAb-EI-L7 to determine whether additional interactions beyond CDR3H contribute to elastase binding. Examination of the HuLys crystal structures suggested that the CDR2H and CDR1L loops are exposed and may be in proximity to the HNE surface (Figure S12). Therefore, two mutants of hAb-EI-L7, hAb-EI-L7-H (W52A, D54A, N56A, and D58A) and hAb-EI-L7-L (N28A,

H30A, and Y32A), were designed by mutating surface-exposed residues to alanine in CDR2H and CDR1L, respectively. Compared with the wild-type hAb-EI-L7, a decrease of potency was observed for both mutants, as measured by the HNE inhibition assay (Figure S13). The K_i values for hAb-EI-L7-H and hAb-EI-L7-L against HNE were 1.16 ± 0.81 and 5.56 ± 1.94 , respectively, corresponding to 1.4- and 6.7-fold decreases of affinities. These data support the notion that the other CDR loops of HuLys make contact with elastase and suggest that it may be possible to further increase potency and selectivity by modifying the structures of these CDRs as well.

Finally, we examined the selectivity of the engineered antibodies to ensure that they are still specific for human elastase. The six hAb-EI Fabs were tested against two other closely related serine protease family members, trypsin and chymotrypsin. These three enzymes share a high degree of similarity in their three-dimensional fold with elastase (Figure S14). As shown in Figure 3D,E, no inhibition was observed between anti-HNE antibodies and the two proteases at concentrations up to $1 \mu\text{M}$. In addition, we demonstrated that mutant Fab hAb-EI-L7-AA, bearing Cys to Ala mutations of both cysteine residues in the CDR3H loop of hAb-EI-L7 (Table 1), loses its ability to bind and inhibit HNE. This result suggests that the disulfide bond is crucial in maintaining the β -hairpin conformation of the long CDR3H loop. Additionally, we determined the inhibitory activity of hAb-EI-L7 against proteinase 3 (PR3), a serine protease closely related to HNE, which shares not only a high sequence similarity but also substrate specificity.²⁵ As shown in Figure S15, hAb-EI-L7 had $K_i > 300 \text{ nM}$ for PR3, which is more than 300-fold less potent compared to its activity against HNE.

In conclusion, we have developed a novel approach to design antibody-based inhibitors against proteases by engineering CDR3H of the antibody's variable region, which afforded potent and selective inhibitors against trypsin and HNE with low nanomolar affinities. In addition, using HNE as an example, we showed that the engineered antibody can be humanized and further optimized to afford a highly potent (sub-nanomolar affinity) and selective human anti-HNE antibody. Currently, an endogenous protein HNE inhibitor, Elafin, is in clinic trials for its effect on the postoperative inflammatory reactions in esophageal cancer surgery, coronary artery bypass surgery, and kidney transplantation, as well as pre-clinical development for several inflammatory conditions/diseases.²⁶ Elafin has high *in vitro* potency against HNE ($K_i = 0.6 \text{ nM}$)²⁷ but suffers from a short half-life that could limit its therapeutic utility. Rationally designed antibody protease inhibitors with comparable potency and superior pharmacokinetic properties may represent a promising alternative.

■ ASSOCIATED CONTENT

🔍 Supporting Information

Experimental details and supporting figures. This material is available free of charge via the Internet at <http://pubs.acs.org>.

■ AUTHOR INFORMATION

Corresponding Authors

*schultz@scripps.edu

*fwang@calibr.org

Notes

The authors declare no competing financial interest.

■ ACKNOWLEDGMENTS

We thank Dr. Xueyong Zhu for guidance with the Octet instrument. This work was supported by funding from the California Institute for Biomedical Research to the Scripps Research Institute.

■ REFERENCES

- (1) Overall, C. M.; Blobel, C. P. *Nat. Rev. Mol. Cell Biol.* **2007**, *8*, 245.
- (2) Ganesan, R.; Eigenbrot, C.; Kirchhofer, D. *Biochem. J.* **2010**, *430*, 179.
- (3) Farady, C. J.; Sun, J.; Darragh, M. R.; Miller, S. M.; Craik, C. S. *J. Mol. Biol.* **2007**, *369*, 1041.
- (4) Duriseti, S.; Goetz, D. H.; Hostetter, D. R.; LeBeau, A. M.; Wei, Y.; Craik, C. S. *J. Biol. Chem.* **2010**, *285*, 26878.
- (5) Ganesan, R.; Eigenbrot, C.; Wu, Y.; Liang, W. C.; Shia, S.; Lipari, M. T.; Kirchhofer, D. *Structure* **2009**, *17*, 1614.
- (6) Ganesan, R.; Zhang, Y.; Landgraf, K. E.; Lin, S. J.; Moran, P.; Kirchhofer, D. *Protein Eng. Des. Sel.* **2012**, *25*, 127.
- (7) Wu, Y.; Eigenbrot, C.; Liang, W. C.; Stawicki, S.; Shia, S.; Fan, B.; Ganesan, R.; Lipari, M. T.; Kirchhofer, D. *Proc. Natl. Acad. Sci. U.S.A.* **2007**, *104*, 19784.
- (8) Farady, C. J.; Sellers, B. D.; Jacobson, M. P.; Craik, C. S. *Bioorg. Med. Chem. Lett.* **2009**, *19*, 3744.
- (9) Schneider, E. L.; Lee, M. S.; Baharuddin, A.; Goetz, D. H.; Farady, C. J.; Ward, M.; Wang, C. I.; Craik, C. S. *J. Mol. Biol.* **2012**, *415*, 699.
- (10) Laskowski, M., Jr.; Kato, I. *Annu. Rev. Biochem.* **1980**, *49*, 593.
- (11) Wang, F.; Ekiert, D. C.; Ahmad, I.; Yu, W.; Zhang, Y.; Bazirgan, O.; Torkamani, A.; Raudsepp, T.; Mwangi, W.; Criscitiello, M. F.; Wilson, I. A.; Schultz, P. G.; Smider, V. V. *Cell* **2013**, *153*, 1379.
- (12) Robinson, J. A. *Acc. Chem. Res.* **2008**, *41*, 1278.
- (13) Brauer, A. B. E.; Kelly, G.; McBride, J. D.; Cooke, R. M.; Matthews, S. J.; Leatherbarrow, R. J. *J. Mol. Biol.* **2001**, *306*, 799.
- (14) Korsinczyk, M. L.; Schirra, H. J.; Rosengren, K. J.; West, J.; Condie, B. A.; Otvos, L.; Anderson, M. A.; Craik, D. J. *J. Mol. Biol.* **2001**, *311*, 579.
- (15) Luckett, S.; Garcia, R. S.; Barker, J. J.; Konarev, A. V.; Shewry, P. R.; Clarke, A. R.; Brady, R. L. *J. Mol. Biol.* **1999**, *290*, 525.
- (16) Hubbard, S. J.; Campbell, S. F.; Thornton, J. M. *J. Mol. Biol.* **1991**, *220*, 507.
- (17) Madala, P. K.; Tyndall, J. D. A.; Nall, T.; Fairlie, D. P. *Chem. Rev.* **2010**, *110*, Pr1.
- (18) Tyndall, J. D. A.; Nall, T.; Fairlie, D. P. *Chem. Rev.* **2005**, *105*, 973.
- (19) Brennecke, P.; Arlt, M. J. E.; Campanile, C.; Husmann, K.; Gvozdenovic, A.; Apuzzo, T.; Thelen, M.; Born, W.; Fuchs, B. *Clin. Exp. Metastasis* **2014**, *31*, 339.
- (20) Equation 9.6, in Copeland, R. A. *Enzymes*, 2nd ed.; Wiley: New York, 2000.
- (21) Korkmaz, B.; Horwitz, M. S.; Jenne, D. E.; Gauthier, F. *Pharmacol. Rev.* **2010**, *62*, 726.
- (22) McBride, J. D.; Freeman, H. N. M.; Leatherbarrow, R. J. *Eur. J. Biochem.* **1999**, *266*, 403.
- (23) Holmes, M. A.; Buss, T. N.; Foote, J. J. *Exp. Med.* **1998**, *187*, 479.
- (24) Kenett, D.; Fleming, G.; Katchalskikatzir, E.; Poljak, R. J. *Mol. Immunol.* **1987**, *24*, 313.
- (25) Hajjar, E.; Broemstrup, T.; Kantari, C.; Witko-Sarsat, V.; Reuter, N. *FEBS J.* **2010**, *277*, 2238.
- (26) Shaw, L.; Wiedow, O. *Biochem. Soc. Trans.* **2011**, *39*, 1450.
- (27) Moroy, G.; Alix, A. J.; Sapi, J.; Hornebeck, W.; Bourguet, E. *Anticancer Agents Med. Chem.* **2012**, *12*, 565.